

Brain Tumor Classification using SLIC Segmentation with Superpixel Fusion, GoogleNet, and Linear Neighborhood Semantic Segmentation

Snehalatha Naik* & Siddarama Patil

Poojya Doddappa College of Engineering, Aiwana-E-Shahi Area, Shambhognlli, Kalaburagi 585 102, Karnataka, India

Received 11 August 2022; revised 22 September 2022; accepted 06 October 2022

Brain tumor is an abnormal tissue mass resultant of uncontrolled growth of cells. Brain tumors often reduce life expectancy and cause death in the later stages. Automatic detection of brain tumors is a challenging and important task in computer-aided disease diagnosis systems. This paper presents a deep learning-based approach to the classification of brain tumors. The noise in the brain MRI image is removed using Edge Directional Total Variation Denoising. The brain MRI image is segmented using SLIC segmentation with superpixel fusion. The segments are given to a trained GoogleNet model, which identifies the tumor parts in the image. Once the tumor is identified, a Convolution Neural Network (CNN) based modified semantic segmentation model is used to classify the pixels along the edges of the tumor segments. The modified semantic segmentation uses a linear neighborhood of the pixel for better classification. The final tumor identified is accurate as pixels at the border are classified precisely. The experimental results show that the proposed method has produced an accuracy of 97.3% with GoogleNet classification model, and the linear neighborhood semantic segmentation has delivered an accuracy of 98%.

Keywords: Border pixels, CNN, MRI, Total variation denoising

Introduction

The human brain is the essential component of the human body, yet occasionally, brain cells have developed unintentionally, which causes severe harm to the brain. Patients with brain tumors are becoming more numerous today. A brain tumor develops inside the skull from a cluster of aberrant cells. Basically, brain tumour can be classified as benign, malignant, or normal.¹ Primary tumour begin in the human brain, where they gradually grow as brain cells, nerve cells, membranes, and glands expand. Secondary brain tumors begin in one area of the body and spread to other areas of the brain. Only the early stages of a brain tumor should be recognized to begin effective treatment. Early therapy can save future brain issues. Diagnostic methods, including MRI scans and CT scans, have been used to distinguish between aberrant and normal cell development in the brain.²

When interpreting brain tumor slices manually based on a doctor's visual assessment, it may be challenging to make the correct diagnosis and time-consuming when examining many MRI brain images. The computer-aided diagnosis system is necessary to overcome the mistakes present in the human-based

diagnostic technique. There are numerous techniques for semi-automatic and automatic picture categorization, but most of them are unsuccessful because medical images frequently contain unknown noise, weak and homogeneous borders, and poor image contrast.^{2,3} Most medical photos have specific intricate structures. Thus, it is essential to classify them accurately for clinical diagnosis. Methods for image processing have been utilized to enhance the efficiency of automated image segmentation, particularly in the segmentation of brain tissue.⁴

Image segmentation is used to identify infected tumor tissues using medical imaging modalities. Segmentation, which is the process of dividing an image into various blocks or sections that share identical and common characteristics like grey level, borders, brightness, contrast, color, and texture, is a crucial and essential stage in the study of images. Medical image segmentation is used to identify brain tumors using MR images or other medical imaging modalities to choose the appropriate therapy at the appropriate time. Several techniques, including the expectation-maximization (EM) algorithm, knowledge-based techniques, artificial neural network (ANN), support vector machine (SVM), and fuzzy clustering methods, have been presented to categorize brain cancers in MR images (FCM).⁵ Region-based

*Author for Correspondence
E-mail: veer9sneha@gmail.com

segmentation is a popular method to segment medical images.

Discriminative clustering and feature selection method has been studied by Kong *et al.*⁶, for brain tumor segmentation. The brain MR images are claimed to be segmented into the CSF, edema, GM, WM, and tumour by Demirhan *et al.*⁷ new tissue segmentation method based on neural networks and wavelets. To effectively classify dynamic contrast-enhanced MR images for addressing various imaging protocols and handling real data nonlinearity, the suggested method uses texture characteristics, SVM, and wavelet transform.⁷⁻¹⁰ According to Torheim *et al.*, the proposed method has produced better predictions and better outcomes for detecting the tumor volume and clinical variables than the first-order statistical features.⁸ The idea of segmenting and categorizing brain tumors using radial basis function (RBF) kernel-based SVM and principal component analysis has been introduced by Kumar and Vijayakumar *et al.*¹¹ (PCA). An effective technique for classifying brain tumors from MR images has been published by Sharma *et al.*¹² This method uses artificial neural networks to construct texture-primitive characteristics as a classifier and segmentation tool (ANN).

Traditional classification methods used in machine learning include pre-processing, feature extraction, feature selection, dimension reduction, and classification. The level of competence in the particular topic typically goes along with the feature extraction. The use of traditional machine learning algorithms is a difficult endeavor for non-experts. Although other fewer methods have been used that exhibit inherent multiple obstacles, deep learning algorithms, notably CNN, have shown their exceptional performance in bioinformatics. ConvNet or CNN have been used as deep machine learning algorithms to analyse the photos.¹³ The important and intriguing patterns and correlations can be extracted from the data using data mining and super pixel segmentation techniques. ML approaches have been demonstrated to be successful and effective for earlier tumor identification and prevention.

A deep learning-based automated brain tumor detection system is presented in this paper. To improve accuracy, semantic segmentation, GoogleNet, and picture segmentation have been combined. The proposed model is designed to classify the segments of the brain MRI as tumor and the

identified tumor segment is finetuned at the edges. This enhances the overall performance of the system.

Proposed Method

This section talks about how the SLIC segmentation model with superpixel fusion receives the input image. Superpixel samples of both tumors and non-tumors are used to train GOOGLNET. The trained GoogleNet model then categorizes the separated superpixels, and the discovered tumour component is subsequently submitted to linear neighborhood semantic segmentation. The suggested model includes many phases:

- **Phase 1:** The suggested superpixel segmentation is used to segment the input brain MRI picture, and CNN will classify the parts it has received.
- **Phase 2:** Segments that are classified as tumors are sent to a modified form of semantic segmentation, which finds tumor pixels.

In Fig. 1 the model for brain tumor detection is presented. The input MRI image is sent to total variation denoising algorithm to remove the noise. The SLIC segmentation is applied to the image to segment the brain MRI into parts. The segments are then classified using GoogleNet. The edge refinement is performed using linear neighborhood semantic segmentation to identify the precise region of the tumor.

Next section presents the image denoising technique using EDTVD.

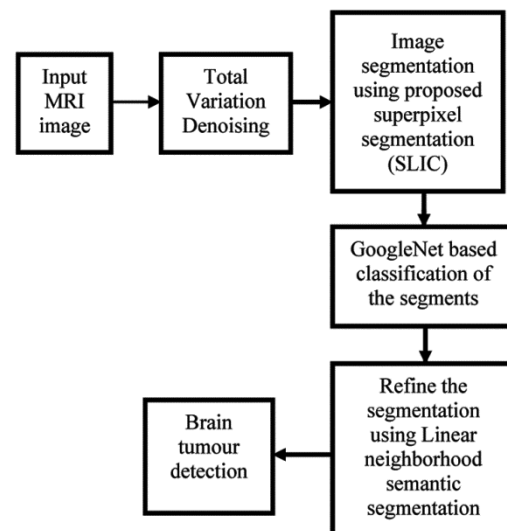


Fig. 1 — Proposed model block diagram

Image Denoising using Edge Directional Total Variation Denoising

The Edge Directional Total Variation De-Noising (EDTVD) is provided with the input MRI image. The estimation of the directions of the edges is done in the image. The estimation of the total variation component is performed depending on the directions of the edges. The final output is obtained by minimizing the TV and Error. The stages included in the proposed method are given in Fig. 2.

A variant of TV has been proposed for increasing the ability of denoising using the DTV algorithm. In this estimation, the purpose of the edge at each pixel is resolved. This improves the viability of the computation by holding the edges present in the image. The basic state of the EDTVD is shown in Eq. (1). The E_{DTV} value is obtained by using the DTV component and the expectation component $E(x, y)$.

$$E_{DTV} = \min_y [\lambda DTV_{\theta}(y) + E(x, y)] \quad \dots (1)$$

And alongside the angle θ , the DTV model improves dispersing while the prominent course when the angle matches with angle θ , the DTV model will redesign the basic structure, or there will be results, beat the structure. It is important to build θ spatially contrasting all during complete picture when there be a couple of dominating headings in the image. In this research work, spatially contrasting $\theta(x, y)$ in perspective on angle heading of image is proposed as shown in Eq. (2).

$$(\theta_x(x, y), \theta_y(x, y)) = (n_1(x, y), n_2(x, y)) \quad \dots (2)$$

Edge directions in the image are $(\theta_x(x, y), \theta_y(x, y))$. The $\theta(x, y)$ coincide regionally

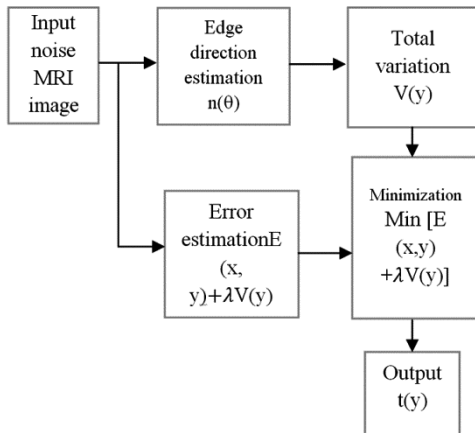


Fig. 2 — Block diagram of proposed method

with image angle bearing. Therefore, the EADTV model is versatile to upgrade dispersion along the picture angle course. The angle heading $(\theta_x(x, y), \theta_y(x, y))$ plays a significant job as well as must be assessed ahead of time. The angle direction be able to measure by image $R(x, y)$ when there be an image $R(x, y)$ as allusion, and might be written as shown in Eq. (3)

$$(\theta_x(x, y), \theta_y(x, y)) = \frac{(-R_y, R_x)}{\sqrt{R_x^2 + R_y^2}} \quad \dots (3)$$

Gradient vector of $R(x, y)$ is (R_x, R_y) . Hence, the numerical method is described and customized by adaptive $\theta(x, y)$ to minimize the EADTV model. Once the image is denoised, the image is sent to superpixel segmentation described in section 2.2. The segmentation divides the image into several parts, and these parts are combined to avoid noise and reduce the processing during classification.

Superpixel Segmentation Algorithm

The image is segmented using the clustering method known as superpixel segmentation. This approach involves performing initialization and refinement schemes up until certain termination requirements are met. A distance function balances the superpixels' features, intensity, and border adherence in this clustering method. The seeds are initially arranged in a hexagonal configuration, and the location of the seeds is at the local pixel value with the lowest gradient. Each pixel in the input image is given a different name based on the associated superpixel.

For the distance calculation, a 5-dimensional vector is used for each pixel $|dl da db dx dy|^T$ set up. The vector $|dl da db|^T$ stands for the pixel color in the CIELAB color space. This three-dimensional color space divides colours based on their hue and brightness ability (black-and-white scale). Color differences can be thought of as distance in this way. The spatial distance on the image is represented by the vector $|dx dy|$. The size of the CIELAB color space and the size of the image determines how far off color values can be from one another. So that both spatial distances have an equal impact on the outcome, the spatial distance must be normalized. Eqs (4–6) show the d_{lab} , d_{xy} and D_s values used in superpixel segmentation.

$$d_{lab} = \sqrt{(dl_k - dl_i)^2 + (da_k - da_i)^2 + (db_k - db_i)^2} \quad \dots (4)$$

$$d_{xy} = \sqrt{(dx_k - dx_i)^2 + (dy_k - dy_i)^2} \quad \dots (5)$$

$$D_s = d_{lab} + \frac{m}{s} d_{xy} \quad \dots (6)$$

where, d_{lab} is the distance between intensity values, d_{xy} is the spatial pixel distance, m is compactness, s is cluster distance

D_s is the sum of distance between intensity values (d_{lab}) and spatial pixel distance d_{xy} normalized with cluster distance s . D_s can be varied with the help of compactness factor m . A larger value of m produces better segmentation.

The segmented picture super pixels are then subdivided into three groups. Depending on its location, a data superpixel may be in a dense area (core superpixel), on its edge (edge superpixel), or in an area with little human habitation (noise superpixel). The area surrounding a pixel is what is meant by the definition of. A little more specifically:

- **Core superpixel:** There are at least MinPixCnt data superpixels in the vicinity of the core super pixel.
- **Edge superpixel:** An edge superpixel is not a core superpixel but lies in the neighborhood of a core superpixel.
- **Intoxication superpixel:** An intoxication superpixel is neither a core nor an edge superpixel.

Informally said, edge super pixels are allocated to the cluster of a corresponding core superpixel, noise superpixel is ignored, and two core super pixels with a distance of no more than land in the same cluster.

Algorithm

Step 1: Name the superpixels as core, edge, or noise superpixels.

Step 2: Delete all noise superpixels.

Step 3: Connect core superpixels that lie within an ϵ - ball with an edge.

Step 4: A lot of connected key superpixels form a separate cluster.

Step 5: Assign each edge superpixel to the cluster of an adjacent core superpixel.

As discussed in the algorithm, the superpixels are first labelled into core, edge and noise. The noise super pixels are merged with the neighbors. The core superpixels lie within an ϵ – ball range. New superpixels are formed based on the merged ones without disturbing the edge super pixels. The

segmented regions are sent to the classification module consisting of GoogleNet. This step classified the tumor in the brain MRI.

GoogleNet

GoogleNet is a deep learning model with 22 layers.¹⁴ GoogleNet shows that it is not necessary to stack the convolutional layer and the pooling layer in sequence.

- **Convolutional layer:** In the Convolutional layer, a filter called a kernel is used for input data to perform a convolution operation. When the input image and the filter are arranged similarly, the numerical value becomes higher by multiplication, and it can be extracted as a feature of the image. By applying various filters, a group of filters that captures the characteristics of various places in each image is completed.
- **Rectified Linear Unit (ReLU):** Conventionally, as a non-linear activation function, $f(x) = \tan(x)$ or $f(x) = (1 + e^{-x})$ was used, $f(x) = \max(0, x)$ learning is accelerated by using Rectified Linear Units (ReLU). This is because it can solve the vanishing gradient problem when the conventional activation function is used in a deep network. ReLU has also been proposed with an improved activation function, but it is widely used as a standard activation function even in the latest models. For the activation function after convolution, ReLU is often used to deal with the vanishing gradient problem. ReLU is a function that outputs a positive value as it is and sets a negative value to 0. After the convolution process, the characteristics of the data appear as large positive values. In the first place, the part that has a negative value is the part that was not filtered as a feature, so there is no problem even if it is set to 0.
- **Pooling layer:** The purpose is to blur the features that emerge in the convolution layer and to make them learn as if they were the same as other similar features. By doing so, it becomes possible to detect the feature even in another image
- **Batch Normalization:** Batch Normalization is mainly in the hidden layer of a convolutional neural network (CNN), after normalizing the features for each channel based on the data distribution in the batch. A differentiable transformation (layer) that performs scale

shifting. Batch normalization can achieve faster and more stable learning convergence while preserving the expressive power of the original CNN. The "batch normalization layer", batch normalization has become a standard component (= layer) in CNN.

The finetuning of the tumor segment is done using semantic segmentation at the edges. This section presents the implementation of semantic segmentation using CNN.

Semantic Segmentation

Image segmentation divides an image into various segments, making it simple to analyse the provided image. Graph partitioning techniques, K-means clustering, image thresholding, the Watershed algorithm, and others are a few strategies that have been employed in the literature. Region-based approaches and free-form areas that are extracted from the image are described using region-based classification. Using a pixel labelling that contains the highest scoring region, region-based predictions are converted into pixel predictions during the test period.

Semantic segmentation, one of the challenging jobs of comprehending the entire scene in computer vision, is one of the main problems. In the recent years, deep learning models have been used extensively in segmentation applications in various fields. Semantic segmentation using CNN is one application that produced better results compared to several existing models.

Fully Convolutional Network-Based Semantic Segmentation

The FCN network pipeline is the traditional CNN extension where pixel to pixel mappings are performed. The traditional CNN is created by considering the input photos of any size. The primary drawback of CNNs is that they can only accept and produce labels from completely linked layers that are fixed for a limited range of input sizes. On the other hand, FCNs (Fig. 3) can make predictions on inputs of any size that just contain pooling and convolutional layers.

The main problem with the FCN is that the output feature maps resolution is down-sampled by propagating via many alternated pooling and convolutional layers. The FCN direct predictions typically have low resolution, which causes rather fuzzy object boundaries. Understanding how semantic segmentation occurs in convolutional networks is crucial. The significant portions of a picture are

determined through semantic segmentation. One can talk about the connections between pixels from one class and those from another class. Consideration is given to the CNN with first layer encoding. Based on describing the image as a mixture of elements like gradients or edges in the fundamental convolution operation, the image is encoded into a higher-level representation. However, although features like edges are not unique, the neighborhood context still applies to them. When back-propagating during decoding and up-sampling, these features have been decoded based on the per-pixel mappings concerning the class relationships.

Linear Neighborhoods Semantic Segmentation

A classification model based on pixels is used in conventional semantic segmentation. The intensity value is used to categories each pixel. The semantic segmentation model faces a thresholding difficulty because the brain MRI picture is in grayscale. Additionally, the intensity of the tumor is mirrored in the skull and brain fluids. A linear neighborhood model is used to get over these problems and find the tumor pixels at the edges of the superpixels. To improve classification accuracy, this model considers the pixels to the left and right of the center pixel when training the CNN model as illustrated in Fig. 4.

In Fig. 4, $Pix(x,y)$ is the current pixel, $Pix(x-1,y)$ is the pixel to the left, and $Pix(x+1,y)$ is the pixel to the right. The pixel group is considered while the CNN model is being trained for semantic segmentation.

Results and Discussion

This section presents the experimental results carried out to validate the proposed model. The results

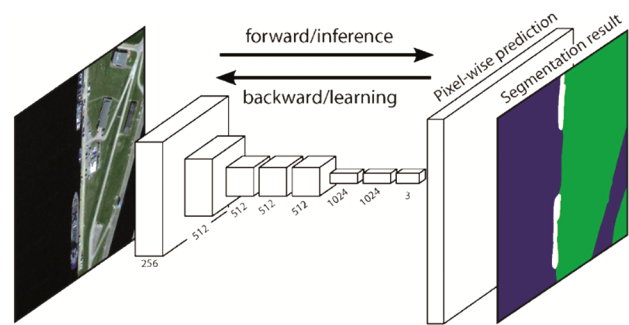


Fig. 3 — FCN Architecture

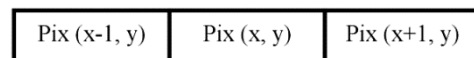


Fig. 4 — Linear neighborhood of the pixel for semantic segmentation

of denoising, classification, and edge finetuning are discussed in this section.

Image Denoising

The proposed methodology is applied on real-time MRI pictures that contain noise. The proposed algorithm kept the edges while removing the noise. Consequently, the picture may be sent for comparable processing, such as classification and segmentation, which can be challenging in noise. The results of the suggested approach and the currently used method are compared, and the MSE and PSNR values are tabulated. The average PSNR generated by the proposed method was 79.24. The Directional TV generated a PSNR of 73.11 while the PSNR for the whole variant was 66.40. Further, Table 1 shows the comparative analysis of the proposed technique with other models.

Brain Tumor Classification

Monitoring the training process is frequently helpful when networks are trained for deep learning. When the 'Plots' parameter in the training Options is set to 'training-progress,' the network will begin training and produce a figure with training metrics for each iteration. Every iteration involves a gradient estimation and a parameter update for the network. The following is shown on the graph:

- Training accuracy — accuracy achieved during the training phase of the data
- Smoothed training accuracy — The accuracy during training with a smoothing filter applied.
- Validation accuracy — accuracy achieved during the validation phase.

The last layer is the cross-entropy layer which acts as the classification layer.

Parameter calculation

True positive (TP) = Images classified correctly as tumor

False positive (FP) = Images classified incorrectly as tumor

True negative (TN) = Images classified correctly as non-tumor

False negative (FN) = Images classified incorrectly as non-tumor

Table 1 — Comparison of Existing and proposed method MSE and PSNR values

	MSE	PSNR
Total Variation	0.015	66.40
Directional Total Variation	0.0032	73.11
Edge Directional Total Variation	0.00078	79.24

Accuracy: accuracy is defined as the number of correctly classified images:

$$Accuracy = \frac{TP+TN}{TP+FP+TN+FN} \quad \dots (7)$$

Sensitivity: Sensitivity determines the number of tumor images correctly classified:

$$Sensitivity = \frac{TP}{TP+FN} \quad \dots (8)$$

Specificity: Specificity determines the number of non-tumor images classified correctly:

$$Specificity = \frac{TN}{TN+FP} \quad \dots (9)$$

The Table 2 shows the parameter calculation for tumour and non tumour classes. The parameters include in the table are true positive, false positive, false negative, true negative, precision, sensitivity, specificity and model accuracy.

GoogleNet performs on the training set accurately and 98.452% of the validation set is classified. The converging of the training set provides good accuracy, and the loss metrics drop to almost zero. However, GoogleNet has proved as a good automatic classifier. The comparative analysis of the proposed model with other existing techniques is given in Table 3. CNN model produced an accuracy of 94.58%. AlexNet produced an accuracy of 97.03%. VGGNet obtained an accuracy of 96.78%. The proposed GoogleNet model produced an accuracy of 98.45% which is higher than all the existing models.

The input image is shown in Fig. 5(a) and Fig. 6(a). The outcome of SLIC segmentation with superpixel fusion is depicted in Fig. 5(b) and Fig. 6(b). The

Table 2 — Parameter calculation

Parameters	Tumor	Non-Tumor
True Positive	24	1095
False Positive	6	25
False Negative	25	6
True Negative	1095	24
Precision	0.80	0.98
Sensitivity	0.49	0.99
Specificity	0.99	0.49
Model Accuracy	98.452%	

Table 3 — Comparative Analysis

Algorithm ^{Ref}	Accuracy
CNN ¹⁵	94.58%
AlexNet ¹⁶	97.03%
VGGNet ¹⁷	96.78%
Proposed GoogleNet model	98.45%

tumour portion recognised by the trained GoogleNet model is shown in Fig. 5(c) and Fig. 6(c). The edge pixels surrounding the segmented tumour are shown in Fig. 5(d) and Fig. 6(d). The dilated area surrounding the tumour boundary is depicted in Fig. 5(e) and Fig. 6(e). The CNN-based linear neighbourhood semantic segmentation model receives the pixels in the dilated boundary region. Fig. 5(f) and Fig. 6(f) display the final image following border pixel classification.

Tumor Finetune Segmentation

The linear neighborhood semantic segmentation's comparative findings are displayed in Fig. 7 and Fig. 8.

In Figs 7 & 8, the output of SLIC segmentation with superpixel fusion is shown in (a); The excised tumour portion is shown in (b); the tumour pixels that were incorrectly classified as such are shown in (c). Green identifies the tumour pixels that were overlooked, and Red represents the non-tumor pixels that were mistakenly labelled as such. The output of the suggested linear neighborhood semantic segmentation technique is finally shown in (d). The

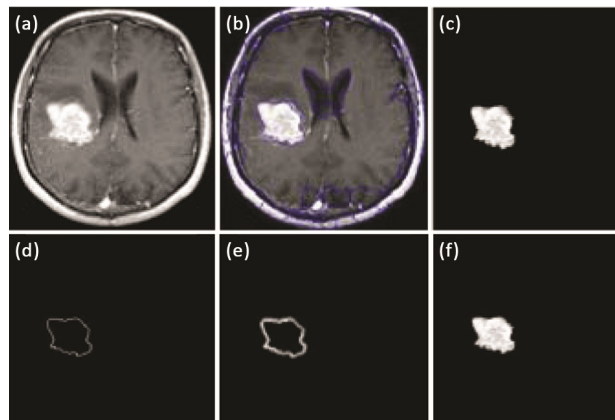


Fig. 5 — Tumor detection steps for input image 1

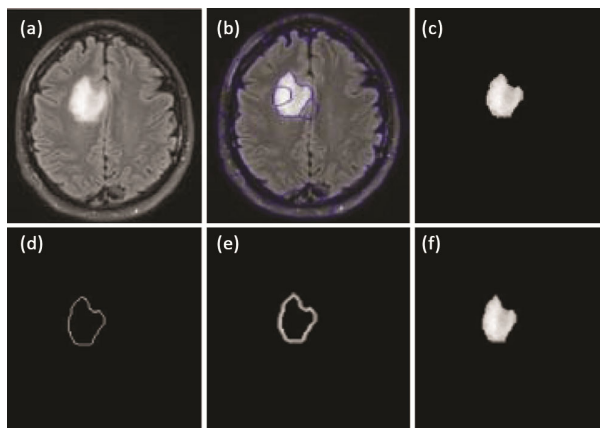


Fig. 6 — Tumor detection steps for input image 2

number of pixels misclassified (shown in red color in Fig. 7(c)) identified as tumor are 179. Number of pixels misclassified as non-tumor (shown in green color in Fig. 7(c)) are 17.

There are 44 pixels that were incorrectly labelled as tumour (indicated in red in Fig. 8(c)). There are 33 pixels that were incorrectly identified as non-tumors (indicated in green in Fig. 8(c)). The MSE comparison results for the existing and suggested approaches are shown in Table 4. The MSE values for

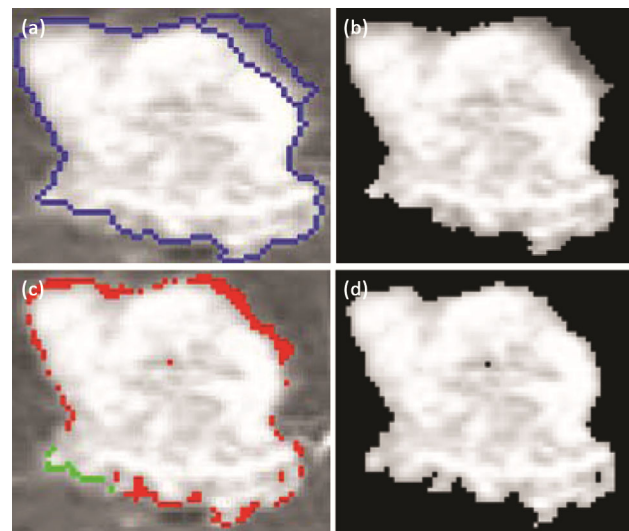


Fig. 7 — Tumor pixel level analysis with (a) Input image 1 SLIC segmentation with superpixel fusion, (b) Input image 1 SLIC tumor segment, (c) Color marked Pixels in the neighborhood of tumor, (d) Linear neighborhood semantic segmentation result

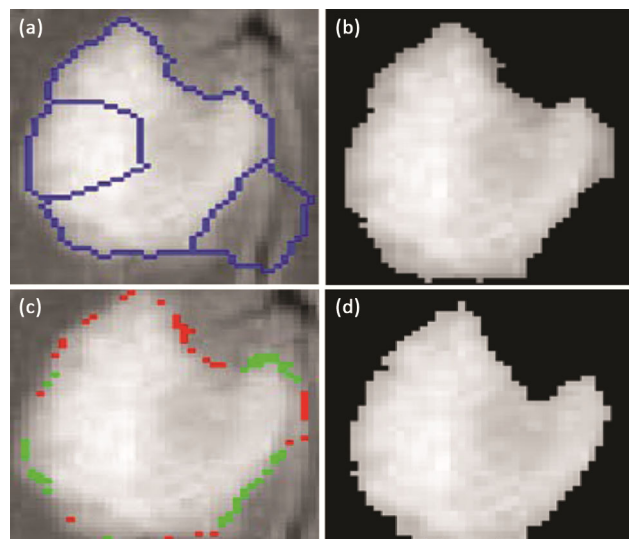


Fig. 8 — Tumor pixel level analysis with (a) Input image 2 SLIC segmentation, (b) Input image 2 SLIC tumor segment, (c) Color marked Pixels in the neighbourhood of tumour, (d) Linear neighbourhood semantic segmentation result

Table 4 — Comparative results of MSE and PSNR

Add title here	Image	K-Means	Mean shift	SLIC	Proposed linear neighborhood semantic segmentation result
MSE	Input image 1	0.0086	0.0054	0.00009	4.5776e-05
	Input image 2	0.0093	0.0043	0.000024	5.3612e-06
PSNR	Input image 1	20.6550	22.6761	40.4576	43.3936
	Input image 2	20.3152	23.6653	46.1979	52.7074

the suggested technique outperform those for K-means, Mean shift, and SLIC.

The PSNR comparison results for the existing and suggested approaches are shown in Table 4. The existing methods of K-means, Mean shift, and SLIC obtained an MSE of 0.0086, 0.0054, and 0.00009 respectively for image 1. The proposed method obtained an MSE of 0.000045 which is much less than the existing methods. Same is the case with image 2. The PSNR values for the suggested technique outperform those for K-means, Mean shift, and SLIC.

The existing K-Means and Mean shift models have obtained PSNR values of less than 25. SLIC produced a PSNR of 40 while the proposed method obtained a PSNR of 43.4 for image 1 and 52.7 for image 2.

Conclusions

Clinicians can identify brain anomalies early in development using MR scans of fetuses. This study presented a three-stage automated brain tumor classification model. SLIC segmentation with superpixel fusion is used to first segment the input image. The trained GoogleNet model is given the segmented super pixels. The linear neighborhood semantic segmentation model accurately classifies the pixels at the border after the GoogleNet model has identified the tumour. The proposed model has produced an accuracy of 98.45%. The experimental findings demonstrate that the borders' pixels cannot be reliably categorized. The suggested model improves classification accuracy by removing non-tumor images and adding tumour pixels.

References

- Iqbal S M, Usman G K, Tanzila S & Amjad R, Computer-assisted brain tumor type discrimination using magnetic resonance imaging features, *Biomed Eng Lett*, **8(1)** (2018) 5–28.
- Abd-E M K, Ali Ismail A, Ashraf A M K & Hesham F A H, A review on brain tumor diagnosis from MRI images: Practical implications key achievements, and lessons learned, *Magn Reson Imaging*, **61** (2019) 300–318.
- Lim K Y & Rajeswari M, A multi-phase semi-automatic approach for multisequence brain tumor image segmentation, *Expert Syst Appl*, **112** (2018) 288 – 300.
- Rundo L, Tangherloni A, Cazzaniga P, Nobile M S, Russo G, Gilardi G M, Vitabile S, Mauri G, Besozzi D & Militello C, A novel framework for MR image segmentation and quantification by using MedGA, *Comput Methods Programs Biomed*, **176** (2019) 159–172.
- Sajid S, Saddam H & Amna S, Brain tumor detection and segmentation in MR images using deep learning, *Arab J Sci Eng*, **44 (11)** (2019) 9249 – 9261.
- Kong Y, Deng Y & Dai Q, Discriminative clustering and feature selection for brain MRI segmentation, *IEEE Signal Process Lett*, **22(5)** (2015) 573–577.
- Demirhan A, Toru M & Guler I, Segmentation of tumor and edema along with healthy tissues of brain using wavelets and neural networks, *IEEE J Biomed Health Inform*, **19(4)** (2015) 1451–1458.
- Torheim T, Malinen E E & Kvaal K, Classification of dynamic contrast enhanced MR images of cervical cancers using texture analysis and support vector machines, *IEEE Trans Med Imaging*, **33(8)** (2014) 1648–1656.
- Guo L, Zhao L, Wu Y, Li Y, Xu G & Yan Q, Tumor detection in MR images using one-class immune feature weighted SVMs, *IEEE Trans Magn*, **47(10)** (2011) 3849–3852.
- Yao J, Chen J & Chow C, Breast tumor analysis in dynamic contrast enhanced MRI using texture features and wavelet transform, *IEEE J Sel Top Signal Process*, **3(1)** (2009) 94–100.
- Kumar P & Vijayakumar B, Brain tumour Mr image segmentation and classification using by PCA and RBF kernel-based support vector machine, *Middle East J Sci Res*, **23(9)** (2015) 2106–2116.
- Sharma N, Ray A, Sharma S, Shukla K, Pradhan S & Aggarwal L, Segmentation and classification of medical images using texture-primitive features: application of BAM-type artificial neural network, *J Med Phys*, **33(3)** (2008) 119–126.
- Nadieh K, Lessmann N, Elise T, Claessens N, Roel D H, Kolk T, Max A V, Benders M J N L & Išgum I, Automatic brain tissue segmentation in fetal MRI using convolutional neural networks, *Magn Reson Imaging*, **64** (2019) 77–89.
- Szegedy, Christian, Liu W, Jia Y, Sermanet P, Reed S, Anguelov D, Erhan D, Vanhoucke V & Rabinovich A, Going deeper with convolutions, arXiv, (2015) 1–9, <https://doi.org/10.48550/arXiv.1409.4842>
- Banerjee S, Sushmita M, Francesco M & Stefano R, Brain tumor detection and classification from multi-sequence MRI: study using ConvNets, *Int MICCAI Brainlesion Workshop*, (2018) 170–179.
- Bhanumathi V & Sangeetha R, CNN based training and classification of MRI brain images, *5th Int Conf Advanced Computing & Communication Systems (ICACCS)*, (2019) 129–133.
- Bingol H & Bilal A, Classification of brain tumor images using deep learning methods, *Turk J Sci Technol*, **16(1)** (2021) 137–143.